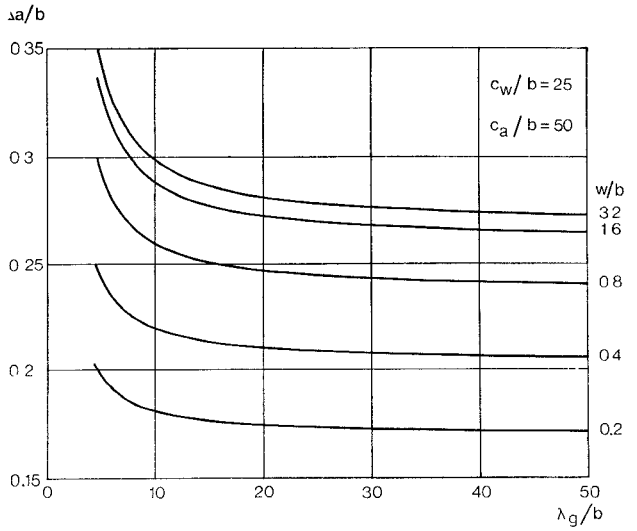

Fig. 3. The foreshortening of a half-wave stripline resonator as a function of the stripline wavelength for some values of the strip width. All dimensions are normalized to the ground-plane spacing.

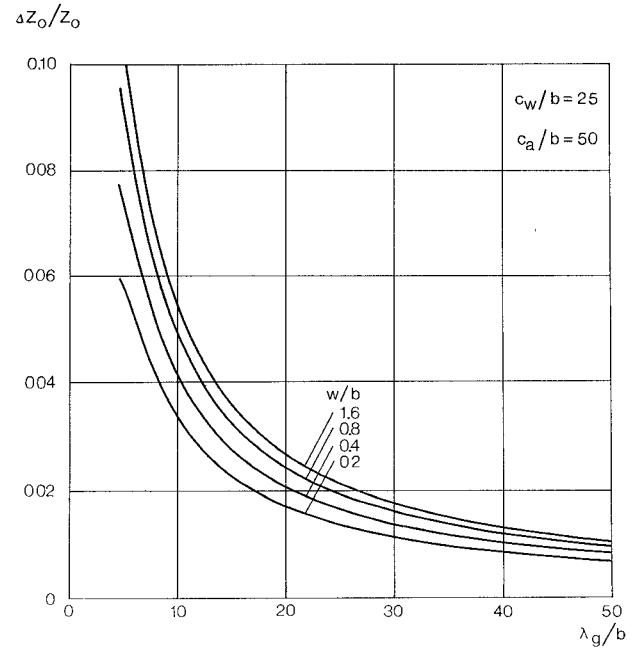

Fig. 4. The relative decrease in the characteristic impedance caused by the end effects of half-wave stripline resonators as a function of the stripline wavelength for some values of the strip width. All dimensions are normalized to the ground-plane spacing.

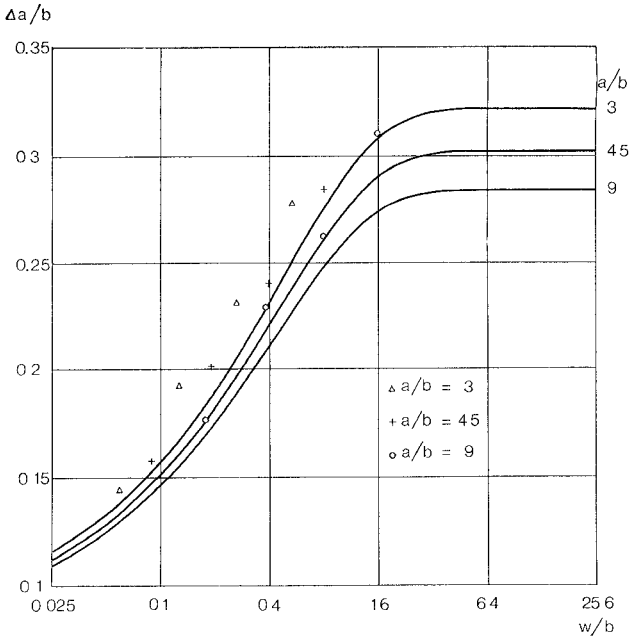

Fig. 5. Measured data points and theoretical curves of the foreshortening as a function of the strip width (logarithmic scale) for some values of the strip length. All dimensions are normalized to the ground-plane spacing.

walls have been moved away far enough so their influence on the results is restricted to the fourth or fifth digit. It is seen that the dynamic foreshortening increases for decreasing resonator length in contrary to the static theory, but is less than the static foreshortening given by (1).

In the diagram in Fig. 4 the relative decrease in the characteristic impedance caused by the end effects is plotted versus the stripline wavelength for some widths of the strips.

The results may also be used for other open-ended stripline configurations, such as $\lambda/4$ stubs, if one takes half the foreshortening in Fig. 3 at every open end of the stripline.

Measurements of the foreshortenings are presented in Fig. 5 together with the corresponding theoretical curves. The foreshortenings have been obtained by measuring the resonance frequencies of stripline resonators. Even if the foreshortening is independent of the relative dielectric constant of the board, the resonance frequency is not. Thus, when we obtain the foreshortenings from the resonance frequencies, the relative dielectric constant is critical. The manufacturer of the stripline board used states that $\epsilon_r = 2.62 \pm 0.05$. The points have been calculated by using the value 2.62. For narrow strips the agreement is good between theory and practice, but for broader strips the difference is greater. This may depend on the assumption that the current on the strip is laminar all the way to its ends. This is true for a narrow strip, but for a wider strip the current bends to the center at the ends of the strip. This bending makes the current path longer, which will contribute to the foreshortening. Measurements on a slotted strip showed less foreshortening, confirming the current bending theory. Contributory reasons for the difference between theory and practice are the uncertainty of ϵ_r (2.65 had been more advantageous), the finite thickness of the strip, and the air spacing between the boards caused thereby.

References

[1] H. M. Altschuler and A. A. Oliner, "Discontinuities in the center conductor of symmetric strip transmission line," *IRE Trans. Microwave Theory Tech.*, vol. MTT-8, pp. 328–339, May 1960.
[2] R. Lagerlöf, "Stripline fed slots," in *Proc. 1971 European Microwave Conf.*, vol. 1, Aug. 1971.
[3] ——, "Optimal design of cavity backed slot antennas," Chalmers Univ. of Technol. Div. of Network Theory, Rep. TR 7203, Mar. 1972.
[4] W. C. Hahn, "A method for the calculation of cavity resonators," *J. Appl. Phys.*, vol. 12, pp. 62–68, 1941.
[5] S. B. Cohn, "Analysis of a wide-band waveguide filter," *Proc. IRE*, vol. 37, pp. 651–656, June 1949.
[6] S. B. Cohn, "Slot line on a dielectric substrate," *IEEE Trans. Microwave Theory Tech.*, vol. MTT-17, pp. 768–778, Oct. 1969.
[7] R. E. Collin, *Field Theory of Guided Waves*. New York: McGraw-Hill, 1960, p. 579.
[8] N. Marcuvitz, *Waveguide Handbook* (M.I.T. Rad. Lab. Ser.), vol. 10. New York: McGraw-Hill, 1951, pp. 218–219.

Maximum Phase-Locking Bandwidth Obtainable by Injection Locking

LENNART GUSTAFSSON, K. INGEMAR LUNDSTRÖM, AND G. H. BERTIL HANSSON

***Abstract*—A simple rule is presented for the determination of the locking region of an oscillator with a general tuning circuit.**

During the last few years a number of articles have treated the theoretical aspects of injection locking [1]–[6]. Reference is often made to an early paper by Adler [7], whereas the basic work by Van der Pol [8] is often neglected. Van der Pol made a thorough study

Manuscript received April 24, 1972; revised November 16, 1972.
L. Gustafsson is with the Division of Network Theory, Chalmers University of Technology, Gothenburg, Sweden.
K. I. Lundström and G. H. B. Hansson are with the Research Laboratory of Electronics, Chalmers University of Technology, Gothenburg, Sweden.

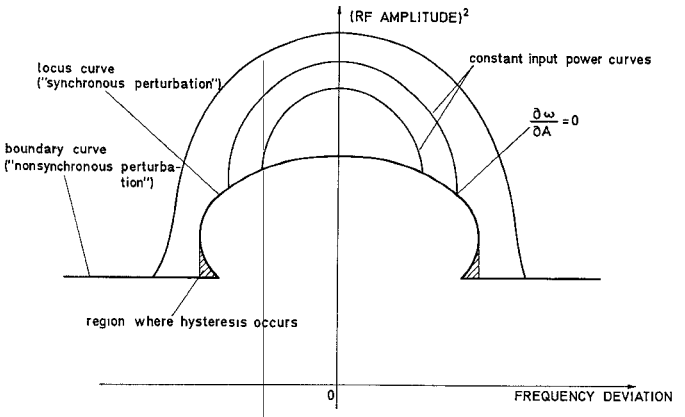

Fig. 1.

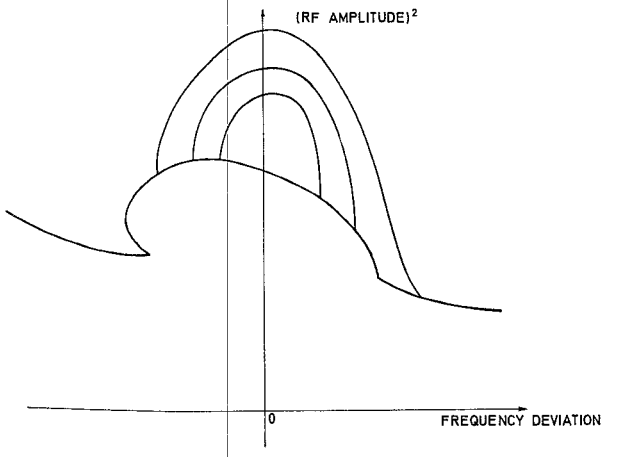

Fig. 2.

of an oscillator consisting of a single-tuned circuit and a third-order nonlinearity. He derived [8, p. 72] the stability borders for this oscillator with an externally applied signal. These stability borders are the same as those given in [5] and [6] for that special case. Van der Pol's method of studying stability could be applied to general tuning circuits and nonlinearities, although this, to our knowledge, has not been done.

In [4] and [5] stability criteria valid for small as well as large injected signals were derived, using a series expansion of the admittance of the active element. Two border lines between stable and unstable locking were introduced, called the boundary and locus curve, respectively, using a notation introduced by Golay [1], who studied the stability of a regenerative single-tuned oscillator. It was pointed out in [1] that the locus curve corresponded to $\partial P_{in}/\partial A = 0$, where P_{in} is the injected power and A the amplitude of the RF voltage across the active element.

In [6] stability was tested by introducing infinitesimal synchronous and nonsynchronous perturbations in the steady-state solution of the voltage across the nonlinear element. These perturbations were then analyzed with the aid of the corresponding incremental input describing function (IIDF). These IIDF's can always be derived from the single sinusoid describing function (DF) which in its first approximation is the same concept as the nonlinear admittance or impedance used in microwave theory. The stability borders are those curves in the amplitude–frequency diagram of the oscillator (Figs. 1 and 2) at which the introduced perturbation will neither increase nor decrease. It was found that the locus curve corresponds to the synchronous perturbation and the boundary curve to the nonsynchronous perturbation. The methods in [5] and [6] yielded results that were identical for small frequency deviations and almost identical for larger frequency deviations. The discrepancy between the results for larger frequency deviations is most likely explained by the fact that a series expansion is done in [5] around the main (injected) frequency, and for larger frequency deviations the "surviving" perturbation will not occur at that frequency and will therefore be determined slightly incorrectly. The main difference between the method of [6] and Van der Pol's [8] is that in [6] the type of perturbation which "survives" at the stability borders and thereby the behavior of the oscillator at the border of stable locking, is also obtained.

The purpose of this short paper is to show that for a general oscillator one of these stability borders—the locus curve—is cut by the constant input power curves where these latter are vertical, i.e., at the maximum obtainable locking bandwidths (for those input powers where such maxima exist) for a certain injected power. Since the remaining stability border—the boundary curve—is very easy to obtain with the aid of the nonsynchronous IIDF, this reduces the computational labor to assess whether a computed stationary state is stable or not.

We restrict our treatment to those cases where the self-oscillation, from which we want to obtain a frequency deviation by means of injection locking, is in itself stable.

To prove the preceding rule concerning the locus curve we first examine the circuit equation for a phase-locked oscillator with a general tuning circuit; the equation [6, eq. 9] is

$$N(A,\omega_1)\frac{G_L T_{12}(j\omega_1)+T_{22}(j\omega_1)}{G_L T_{11}(j\omega_1)+T_{21}(j\omega_1)}=\frac{I_e}{A}\exp(j\theta)\frac{1}{G_L T_{11}(j\omega_1)+T_{21}(j\omega_1)} \quad (1)$$

where N is the describing function (DF) of the nonlinear active element, A is the RF voltage across that element, ω_1 is the frequency of the injected current, G_L is the load, T_{11}, T_{12}, T_{21}, and T_{22} are the elements of the voltage–current transmission matrix for the linear tuning circuit, I_e is the amplitude of the injected current, and θ is the phase difference between the injected current and the RF voltage across the nonlinear element. N may be regarded as the nonlinear admittance of the active element for a single-frequency RF voltage. No restrictions on the nature of the active element are made—it may contain nonlinear conductances as well as nonlinear susceptances, e.g., of the kind caused by the transit time effects in avalanche diodes.

The study is restricted to the stability of single-frequency operation; this is implicit in (1) where only one frequency ω_1 is included. The bias circuit is assumed to be ideal, otherwise an equation determining the variation in bias level should be introduced.

It is easily seen that (1) can be written in the following way

$$N_{re}+jN_{je}+G_e+jB_e=\frac{I_e}{A}\exp(j\theta) \quad (2)$$

where

$$N_e=N_{re}+jN_{je}=N(A,\omega_1)(G_L T_{12}(j\omega_1)+T_{22}(j\omega_1))$$

and

$$G_e+jB_e=G_L T_{11}(j\omega_1)+T_{21}(j\omega_1).$$

From (2) we obtain

$$A^2((N_{re}+G_e)^2+(N_{je}+B_e)^2)=I_e^2 \quad (3)$$

and

$$\tan\theta=\frac{N_{je}+B_e}{N_{re}+G_e}. \quad (4)$$

For a constant injected amplitude I_e but varying frequency, we find

$$\frac{\partial A}{\partial\omega}=-\frac{A\left((N_{re}+G_e)\left(\frac{\partial N_{re}}{\partial\omega}+\frac{\partial G_e}{\partial\omega}\right)+(N_{je}+B_e)\left(\frac{\partial N_{je}}{\partial\omega}+\frac{\partial B_e}{\partial\omega}\right)\right)}{(N_{re}+G_e)^2+(N_{je}+B_e)^2+A\frac{\partial N_{re}}{\partial A}(N_{re}+G_e)+A\frac{\partial N_{je}}{\partial A}(N_{je}+B_e)}. \quad (5)$$

We now test the stability of the locked oscillator with a synchronous perturbation, i.e., a perturbation with frequency ω_1. At the border of stable locking we have from [6, eq. (11) and (12)]

$$N_{re}+jN_{je}+\frac{A}{2}\left(\frac{\partial N_{re}}{\partial A}+j\frac{\partial N_{je}}{\partial A}\right)(1+\exp(j\Phi))+G_e+jB_e=0 \quad (6)$$

where Φ is an angle, the physical meaning of which is unimportant in this context, since we will eliminate it.

$$N_e+\frac{A}{2}\frac{\partial^N e}{\partial A}(1+\exp(j\Phi))$$

is the IIDF for a synchronous perturbation. Separating (6) into real and imaginary parts and eliminating Φ yields

$$(N_{re}+G_e)^2+(N_{je}+B_e)^2+A\frac{\partial N_{re}}{\partial A}(N_{re}+G_e)+A\frac{\partial N_{je}}{\partial A}(N_{je}+B_e)=0. \quad (7)$$

We observe that the border of stable locking determined by a synchronous perturbation is equivalent to

$$\frac{\partial A}{\partial \omega}=\infty \quad \text{or} \quad \frac{\partial \omega}{\partial A}=0$$

from (5).

This means that if A is plotted versus ω for a constant injected amplitude I_e, the locking becomes unstable just at the maximum frequency deviation (in those cases where such a maximum deviation exists); this was implicit in [4]–[6] but not explicitly stated. Note that we have no restrictions on the injected amplitude I_e or the frequency deviation, still the maximum frequency deviation determines a stable state, as long as such a maximum exists and lies in the region which is indicated as stable by the boundary curve(s). In view of the above we can restrict our study of stability to the use of nonsynchronous perturbations, which is usually an exceedingly simple matter; the border of stability is determined by [4, eq. (14) and (15)]:

$$N_{re}+G_e+\frac{A}{2}\frac{\partial N_{re}}{\partial A}=0 \quad (8)$$

$$N_{je}+B_e+\frac{A}{2}\frac{\partial N_{je}}{\partial A}=0. \quad (9)$$

The above discussion is illustrated in Figs. 1 and 2 where typical stability border curves are drawn for oscillators having nonlinear conductance and both nonlinear conductance and susceptance, respectively.

Van der Pol was aware of the rule concerning the locus curve for the particular oscillator which he studied. Since his method does not, however, allow for separation into different kinds of perturbations, this insight could not be practically applied.

The boundary curve is not necessarily single valued. It is, for instance, quite possible to have an oscillator which becomes stably locked when the amplitude crosses the lower boundary curve and then becomes unstably locked again if the injected power is increased so that the amplitude crosses the upper boundary curve.

It is to be noted that whereas the curves for constant injected amplitude are vertical at their intersections with the stability border determined by the synchronous perturbation ("the locus curve"), no such relationship exists regarding the stability border determined with nonsynchronous perturbations ("the boundary curve").

Our discussion has related to amplitudes; it is easily shown that identical relations can be established for the phase θ (i.e., $\partial\omega/\partial\theta=0$ at the border of stable locking determined by a synchronous perturbation). Concerning the output power it should be noted that $\partial A/\partial\omega\rightarrow\infty$ (synchronous stability border) corresponds to $\partial P_{out}/\partial\omega\rightarrow\infty$ provided that

$$N_{re}A+\frac{A^2}{2}\frac{\partial N_{re}}{\partial A}\neq 0.$$

Finally, it should be noticed that for an oscillator having a nonlinear susceptance it is very likely that the power required to bring an unlocked oscillator to a locked state for some frequencies exceeds that required to keep a locked oscillator in a locked state at the same frequencies. Our results pertain to the latter case. No information about the additional power required in the former case can be obtained by the use of synchronous and nonsynchronous perturbations.

The following simple rule has thus been established for the determination of the stable locking region ("holding" region) of an oscillator with a general tuning circuit. If, for a given injected amplitude, there exist points where $\partial\omega/\partial A=0$, these points determine the locking range, unless these points lie in the region which is unstable as determined by a nonsynchronous perturbation (8) and (9). This is valid irrespective of the magnitude of the frequency deviation from the free-running frequency. It should perhaps be pointed out that the technique described here can be used to study amplifiers as well, since the describing function introduced also describes an amplifier.

References

[1] M. J. E. Golay, "Normalized equations of the regenerative oscillator—Noise, phase-locking, and pulling," *Proc IEEE*, vol. 52, pp. 1311–1330, Nov. 1964.
[2] L. J. Paciorek, "Injection locking of oscillators," *Proc IEEE*, vol. 53, pp. 1723–1727, Nov. 1965.
[3] K. Kurokawa, "Some basic characteristics of broadband negative resistance oscillator circuits," *Bell Syst. Tech. J.*, vol. 48, pp. 1937–1955, 1969.
[4] G. H. B. Hansson and K. I. Lundström, "Phase locking of negative conductance oscillators," in *Proc. 1971 European Microwave Conf.*, pp. A6/4: 1–4.
[5] ——, "Stability criteria for phase-locked oscillators," *IEEE Trans. Microwave Theory Tech.*, vol. MTT-20, pp. 641–645, Oct. 1972.
[6] L. Gustafsson, G. H. B. Hansson, and K. I. Lundström, "On the use of describing functions in the study of nonlinear active microwave circuits," *IEEE Trans. Microwave Theory Tech.*, vol. MTT-20, pp. 402–409, June 1972.
[7] R. Adler, "A study of locking phenomena in oscillators," *Proc IRE*, vol. 34, pp. 351–357, June 1946.
[8] B. Van der Pol, "Forced oscillations in a circuit with nonlinear resistance," *Phil. Mag.*, vol. 3, pp. 65–80, Jan. 1927.

Broad-Band Twisted-Wire Quadrature Hybrids

R. E. FISHER

***Abstract*—A symmetrical 3-dB quadrature hybrid, consisting chiefly of a bifilar pair of twisted wires, is described. A cascade of two such hybrids can achieve an octave bandwidth with a 0.7-dB coupling error. Since this class of hybrid is simple, compact, and low in cost, its use may be preferred over the more common coaxial line or printed-circuit types in the frequency region below 1 GHz.**

I. Introduction

The concept of using twisted wires wrapped upon ferrite toroids to form compact, asymmetric, 180° hybrids was first introduced by Ruthroff [1]. It has also been found by several other investigators [2]–[4] that twisted-wire structures can be made to function as *symmetric*, 3-dB quadrature (90°) hybrids, thus permitting the construction of compact directional couplers at arbitrarily low frequencies.

Examples of twisted-wire quadrature hybrids centered at approximately 7 and 300 MHz are shown schematically and pictorially in Figs. 1, 2, and 5. For both hybrids, the coupling section consists of two strands of insulated copper magnet wire tightly twisted together to form a bifilar pair. For the 7-MHz hybrid shown in Fig. 2, the pair is wrapped upon a small ferrite toroid which is then soldered to four BNC along with two mica capacitors. For the 225–400-MHz two-stage hybrid shown in Fig. 5, where much less inductance is required, the wire pairs are bent into loops, and then soldered onto an epoxy fiberglass circuit board along with four omni-spectra-miniature (OSM) connectors.

II. Single-Stage Hybrid Design

Consider Fig. 1. If terminal 1 is connected to terminal 2, and terminal 3 is connected to terminal 4, the resulting two-terminal network is now simply a lumped inductance L, since the magnetic coefficient of coupling between the twisted wires is nearly unity.

If terminal 1 is connected to terminal 4, and terminal 2 is connected to terminal 3, this different two-terminal network can be approximated by a lumped capacitor C, which is the sum of the interwinding capacitance and the external capacitors. At UHF, the external capacitors may not be required.

The 4-port will display hybrid properties when

$$Z_0=\sqrt{\frac{L}{C}}. \quad (1)$$

Equal power division between ports 2 and 4 will occur at a frequency f_0 where

$$\omega_0 L=\frac{1}{\omega_0 C}=Z_0$$

$$\omega_0=2\pi f_0. \quad (2)$$

The transducer loss between ports 1 and 2 is

$$\frac{P_1}{P_2}=1+\left(\frac{\omega_0}{\omega}\right)^2 \quad (3)$$

Manuscript received May 1, 1972; revised November 8, 1972.
The author is with Bell Laboratories, Whippany, N. J. 07981.